

E-ISSN: 2788-9270
 P-ISSN: 2788-9262
www.pharmajournal.net
 NJPS 2023; 3(1): 115-125
 Received: 20-01-2023
 Accepted: 04-03-2023

Sai Sambit Nayak
 Pundit Ravishankar Shukla
 University, Raipur,
 Chhattisgarh, India

Rajendra K Jangde
 Pundit Ravishankar Shukla
 University, Raipur,
 Chhattisgarh, India

Formulation and design optimization of repaglinide loaded transferosomes for management of type II diabetes mellitus

Sai Sambit Nayak and Rajendra K Jangde

DOI: <https://dx.doi.org/10.22271/27889262.2023.v3.i1b.76>

Abstract

Background: An anti-diabetic drug called Repaglinide is used to treat type II diabetes. Repaglinide, a lipophilic medication with a short (1 h) half-life and little solubility in water is classified as a class II biopharmaceutical chemical (BCS) chemical. Only around 55% of drugs with a high metabolism in the first pass are bioavailable orally.

Objective: The development of repaglinide-loaded transferosomes was the key objective of the current study in order to boost transdermal bioavailability.

Method: Thin Film Hydration technique was used to create the transferosomes.

Results: SEM examination revealed that the majority of the transferosomes containing repaglinide had spherical forms. Deformable vesicle formulations were found to have an entrapment efficacy of 68.8% to 87.41%. The F9 formulation has high entrapment efficiency (maximum 87.41%). Transferosomes were discovered to improve the release, according to studies on *in vitro* release. Stability tests for transferosomes were carried out over a three-month period to look at how various levels of temperature affected the total amount of medication entrapped and destroyed, the uniformity of the content, and the physical appearance.

Conclusions: Finally, it may be inferred from the available data that transferosomes were a viable option for transdermal distribution, to extend the release and to enhance site specificity of the medication repaglinide.

Keywords: Transdermal delivery system, transferosomes, repaglinide, type II diabetes mellitus

Introduction

The one of among the most extensively researched illnesses, diabetes mellitus is a severe global fitness issue that is characterized by hyperglycemia and caused by abnormalities in insulin production, insulin function, or both^[1, 2]. There are two distinct forms of diabetes. In the condition known as type 1 diabetes mellitus, which contributes to the autoimmune annihilation of pancreatic beta cells or the requirement for exogenous insulin for patients, beta cells, the body's immune system, outside influences, and genetics interact with one another. Obesity, insulin resistance, and functional flaws in beta cells are all linked to type 2 diabetes mellitus. Normal or high basal insulin levels can be seen as a compensating mechanism for insulin resistance in the early stages of the disease^[3]. A sizable amount of the functional beta cell mass is lost when type 2 diabetes progresses from prediabetes to established disease. While type 2 diabetes more typically affects older persons, type 1 diabetes mellitus frequently manifests in children and young adults^[4]. Throughout the world, 382 million people, about 8.3% of adults, are deemed to have hyperglycemia. 80% of people reside in developing and middle-income nations. One in ten adults, or approximately 592 million people, will develop diabetes by 2035 if these trends continue^[5]. The age of beginning of diabetes mellitus has changed in recent years, with younger people now being disproportionately impacted. Globally, 28 million women are expected to have diabetes mellitus at the moment. Most of these women develop diabetes mellitus of type 2^[6].

Epidemiology

There were 463 million diabetics worldwide as of 2019 (8.8% of the adult population); the majority of cases (almost 90%) were type 2 diabetes^[7]. Male and female rates are comparable^[8]. Rates are expected to rise, according to current trends^[8]. One's risk of passing away young is at least doubled by having diabetes^[9]. In 2019^[9], diabetes was a factor in nearly 4.2 million deaths. It ranks as the sixth most frequent cause of death globally^[10, 11].

Corresponding Author:
Sai Sambit Nayak
 Pundit Ravishankar Shukla
 University, Raipur,
 Chhattisgarh, India

It has been estimated that diabetes-related healthcare expenses will amount to the global economy \$727 billion in 2017 [12]. Nearly \$327 billion was spent in the US on diabetes in 2017 [13]. Spending on medical care is on average 2.3 times higher for diabetics [14]. Taking onto account the global diabetes epidemiology research from the International Diabetes Federation, the 7th edition of the IDF Diabetes Atlas estimates about 415 million adults around the world, corresponding to a total population of 4.72 billion, will suffer from diabetes. As a consequence, one out of eleven adults have the the condition. Out of the projected worldwide population, this number is anticipated to grow to 642 million. By 2040, 6.16 billion people in general, or one in ten, will have hyperglycemia. The Western Pacific region, which comprises of 27 countries, was placed fourth in terms of the prevalence of diabetes by region in 2015, according to the World Health Organisation, with 8.8% (7.7%-10.8%) of the population having the disease. In 2040, South-East Asia will surpass the Western Pacific region, rising to take fifth place with 9.0% (7.3%-11.6%), according to predictions [14]. According to the Annual Health and Morbidity Report 2015, which has been released by the Malaysian Ministry of Health, the incidence of both known and unknown diabetes among those 18 and older was 17.5% (95% CI: 16.6, 18.3) in 2015. Malaysia is a nation in the Western Pacific. One out of every five adults in Malaysia has diabetes [14]. In Malaysia, between 40% and 60% of the population die due to diabetes until they turn 60 [14]. Diabetes claimed the lives of 5 million people worldwide in 2015 [15]. Long-term organ damage or failure is far more likely when there is chronic hyperglycemia, the primary clinical manifestation of diabetes. The most severely affected organs are the blood arteries, kidneys, heart, nervous system, eyes, and kidneys. T2DM often has higher rates of microvascular and macrovascular problems [16].

Repaglinide

Repaglinide is an anti-diabetic medication for the treatment of type II diabetes [17, 18]. Repaglinide is a biopharmaceutical categorization system (BCS) class II chemical that has a short (1 h) half-life and poor water solubility (lipophilic drug, log P=3.97) [19]. The oral bioavailability of substances having a high metabolism in the first pass is only around 55% [20, 21]. We suggested transdermal administration of repaglinide employing transferosomes as a carrier using Soya Lecithin and Span 80 to address these difficulties. Transdermally, the transferosomes can resolve the problem of skin permeability brought on by the stratum corneum's physical barrier [22-24]. Drug-loaded lipid core particles stabilised by a surfactant shell make up transferosomes. High drug penetration in the epidermal layer may be facilitated by transferosomes' nanosize, high surface area, and occlusive effect (hydration) [25-27].

Transferosomes

Specifically created transferosomes are vesicular carrier systems having an activator of edges and a minimum of a single inner aqueous compartment enveloped by a bilayer of lipids. These aqueous, lipid-coated ultra-deformable vesicles have the capacity for self-optimization and self-regulation [28, 29]. Transferosomes may bend and compress themselves through skin constrictions or minuscule holes that are substantially smaller than the dimensions of the vesicles without suffering any appreciable loss due to their natural

elasticity [30, 31]. Instead of the natural or artificial phosphatidylcholine found in conventional liposomes (such as egg phosphatidylcholine (EPC), soybean phosphatidylcholine (SPC), or dipalmitoyl phosphatidylcholine (DPPC)), the altered liposomal vesicular structure (transferosomes) comprises a combination of a phospholipid component and single-chain phosphatidylcholine. Edge activators (EAs), which operate as membrane destabilizing agents, are particularly effective at increasing the deformability of vesicle membranes. This mixture makes the transferosomes bendable and ultra-flexible, boosting their capacity for permeation [32, 33, 34, 35] when coupled in the optimum ratio with the proper lipid. Because they are capable of passing through pores that are substantially smaller than their own sizes, transferosomes have the ability to circumvent the fundamental shortcomings of traditional liposomes. Furthermore, the transferosomes retained their dimensions against breakage despite traversing the tiny gaps. The transfersomal formulation outperforms traditional liposomes because EAs are employed [35]. By including EAs into transfersomal formulations to make hydrophobic medications soluble, drug entrapment effectiveness can be increased. structure of a transferosome. These highly flexible vesicles, which have an aqueous core and a lipid bilayer on top, may regulate and optimise their own behaviour [35]. As opposed to traditional liposomes, which are contained normal, (for example, egg phosphatidylcholine-EPC and soybean phosphatidylcholine-SPC) or manufactured, (for example, dimyristoyl phosphatidylcholine-DMPC, dipalmitoyl phosphatidylcholine-DPPC and dipalmitoyl phosphatidyl glycerol-DPPG) phospholipids [36], the modified liposomal vesicular arrangement (transferosomes) is created out of a phospholipid part and single-chain surfactant compounds as an activator of the edge [36].

When coupled in the right combination with the correct lipid, edge activators (EAs) work astonishingly well as membrane-destabilizing agents that enhance the flexibility of vesicle walls. The combination makes the transfersomes ultra-flexible and malleable, which increases their capacity for permeation [36]. Transferosomes can thereby circumvent the main limitations of conventional liposomes by going through gaps that are significantly smaller than their own diameters. Furthermore, the transfersomes retained their diameters against splitting even after getting through the smaller pores. The transfersomal formulation has improved performance over traditional liposomes as a result of the use of EAs [36].

The EAs used in transfersomal formulations can also help hydrophobic medicines become soluble, improving the formulations' ability to entrap pharmaceuticals [36-37]. The EAs may also fluidize and solubilize the skin lipids, enhancing skin penetration [38, 39]. The result depends on the kinds and volumes of EAs applied during skin permeations. One of the numerous different compounds that work as activators of edges and penetration boosters is surfactant [40]. They have been identified as amphiphilic compounds, which feature a hydrophilic head unit coupled to a fatty aliphatic group [41]. Anionic surfactants frequently enhance skin absorption compared to cationic surfactants, for instance, and they also have a lower critical micelle concentration. However, nonionic surfactants with an uncharged polar head group are more acceptable than cationic and anionic surfactants [41]. Nonionic surfactants are

thought to be less aggressive, hemolytic, and irritating on biological walls. Furthermore, they typically keep the pH of a solution within physiological levels. They also serve as emulsifiers, solubilizers, and potent the protein P-g inhibiting agents, all of which are beneficial for enhancing drug absorption and concentrating on certain tissues^[41]. It is commonly known that trans ferosomal formulations are an important mechanism for the "transdermal delivery" of a range of medicinal medications and are frequently utilised in "transdermal immunization" and "peripheral medication targeting"^[42]. It is generally known that transferosomes have a better than 50% transport efficiency when moving hydrophilic and lipophilic molecules, as well as low and large molecular weight (200 MW 106) bioactive substances, through the skin. Important molecular relationships among the inner and outermost layers of the epidermis are hindered by the different cell organization of the epidermis. Even water cannot penetrate the epidermis faster than 0.4 mg/cm²/h. as transcutaneous permeability rates were studied for compounds with molecular weights ranging between 18 Da (water) to 750 Da (drugs), it was shown that the transferosomes proved capable of transporting these pharmaceutical compounds across the barrier of the skin by in excess of fifty percent in contrast with the untrapped medication^[42]. The maximum transcutaneous permeation rates for these compounds ranged from 0.1 g/h/cm² to 1 g/h/cm². Furthermore, it has been demonstrated that the efficiency of transferosomes in transferring fatty fluorescent tags through the skin of mice is greater than 50%^[42]. A range of solubilities for transferosomes are produced by the hydrophilic and lipophilic components that are present within the vesicle architecture^[43, 44]. Deeper epidermal layers cannot be accessed by vesicles larger than 600 nm, although vesicles smaller than 300 nm can^[45, 46]. However, the dermal and viable epidermal layers of the skin displayed the most content deposition in vesicles with a 70 nm diameter. Additionally, it has been shown that skin penetration was statistically higher for 120 nm transferosomes in comparison to bigger ones^[47]. These novel transfersome delivery techniques also guarantee the optimal distribution, higher bioavailability, and potential durability of phytoactives in herbal formulations^[48]. So, to possibly offer skin care and a range of medical benefits, herbal components may be enclosed in transferosomes^[48]. Transferosomes have been demonstrated to be able to deliver therapeutic compounds into deeper skin layers, establish skin drug depots for a prolonged drug release, and transport medicines into the systemic circulation due to their extensive skin penetration capacities^[49]. Transferosomes thus present a potential chance to introduce a completely new perspective for the judicious distribution of pharmaceuticals^[50].

Materials

Chemicals and reagents

Repaglinide was received as gift from M/s Chromo Laboratories India Pvt. Ltd, Sangareddy Dist, Telangana State, India. Phospholipid (Soya Lecithin) obtained from Central Drug House (P) Ltd., New Delhi, India, Span 80 from Pallav Chemicals & Solvents Pvt. Ltd., Tarapur, India, Methanol from Avantor Performance Material India Limited, Thane, India, Chloroform from LOBA Chemie Laboratory Reagents & Fine Chemicals, Mumbai, India, Phosphate Buffer (P^H 7.4) from Avantor Performance

Material India Limited, Thane, India.

Experimental Design for Optimization

- An analysis technique known as a Box-Behnken Design (BBD) with three parts and a total of three levels was utilized to connect both independent and dependent variables.
- The seventeen runs of BBD were recorded utilizing the data analysis framework Design-Expert software, version 11 (Stat- Ease, Inc., Minneapolis, MN).

Responses like % Particle Size (; R1) and Zeta Potential (R2) of Repaglinide were chosen as dependent factors, whereas phospholipid (A), surfactant (B), and sonication time (C), each at three levels, were chosen as independent variables.

Table 1: Independent variables along with their levels and constraints:

Name	Units	Low	High
Phospholipid	mg	30	70
Surfactant	mg	15	30
Sonication time	min	4	10

Table 2: Dependent variables:

Name	Units
Particle Size	Nm
Zeta Potential	mV

Method

Thin film hydration method

The sacs were created using the thin-film hydration technique. In a combination of solvents, drug, phospholipid, and Span 80 were solubilized. A rotary evaporator was then used to allow the organic solvent to evaporate at 40 °C under decreased pressure. In order to completely evaporate the organic solvents, the chamber was subsequently set in a desiccator with a vacuum for the duration of the night. This caused a thin fatty layer to develop on the flask sidewalls. The mixture was subsequently exposed to phosphate buffer solution (PBS; PH 7.4) at 37 °C in order to hydrate the fatty film. The resulting suspension was well mixed by vortexing for 2 minutes, and the lipid film was completely hydrated by incubating the mixture for 2-3 hours at room temperature^[51].

Morphology of Transferosomes by Scanning Electron Microscopy (SEM)

The transferosomes' form and size were identified using scanning electron microscopy (SEM). A single drop of the formed transferosomes was stained by adding uranyl acetate (2% w/w) on a grid of copper and letting it sit for a while to dry. The colored transferosome samples were air dried before SEM analysis^[52].

Determination of Percentage Entrapment Efficiency (EE %)

Entrapment efficiency was assessed by centrifuging the Transferosomes sample (1 ml in PBS) in an Eppendorf for a period of time at 15000 revolutions per minute and collecting the resulting supernatant. The obtained supernatant's free quantity of drugs (Cf) was analysed using UV-visible spectroscopy (Shimadzu UV-1800, Japan), and the EE% was determined using the following formula:

$$\text{Entrapment Efficiency (EE \%)} = \frac{C_t - C_f}{C_t} \times 100$$

Where, C_t = drug concentrations overall, and,
 C_f = levels of the freely available medication [53].

Particle Size, Polydispersity Index, and Zeta Potential: Zetasizer-Pro (Malvern Equipment GmbH, Herrenberg, Germany) was used to determine the particle size and polydispersity index of the produced unloaded and drug-loaded Transferosomes. The substances were maintained at a constant degree of 25 °C after being suitably diluted in screened phosphate buffer saline. During the laser light scattering screening, a laser beam with an emission wavelength of 635 nm was focused at a dissipation angle of 90°. The surface charge of drug-entrapped vesicles was determined using the Zetasizer (Malvern Equipment GmbH, Herrenberg, Germany). One milli litre of transferosomal fluids has been diluted with ten millilitres of double-distilled water in order to calculate the vesicles' typical zeta potential [54].

Loading Capacity

Using the ultracentrifugation technique, the amount of medication integrated into the lipid matrix was calculated. The prepared Transferosomes were dispersed in centrifuge tube at 15000 rpm for 1 hour, the supernatant (1 ml) pipette out and diluted with phosphate buffer (pH 7.4). The un-entrapped complex was determined by U.V spectrophotometer at 285 nm. The drug loading capacity (LC) is calculated by following formula:

$$\% \text{ LC} = (W_1 - W_2) / (W_1 - W_2 + W_3) \times 100$$

Where,

W1 = the amount of medication injected into the body

W2 = the drug weight in the supernatant

W3 = the amount of fat added to the system, in weigh

In vitro Drug Release Study

- By membrane bag method:
- Through the egg membrane, a release study of Transferosomes loaded with Repaglinide was conducted.
- The membrane was positioned in-between the donor and receptor compartments.
- The membrane surface of the donation chamber received 1 ml of the transferosomal solution. The space for receptors was filled with 125ml of pH 7.4 phosphate buffer.
- Throughout the experiment, the solution being used on the receptor side was kept around 37 °C and rotated magnetically at 100 rpm.
- Hourly samples from the receptor compartment were collected right away and replaced with a comparable quantity of fresh buffer solution to sustain the sink situation.

- Repaglinide was detected in the samples obtained using spectrophotometric analysis at a wavelength of 285 nm [55].

Stability Study

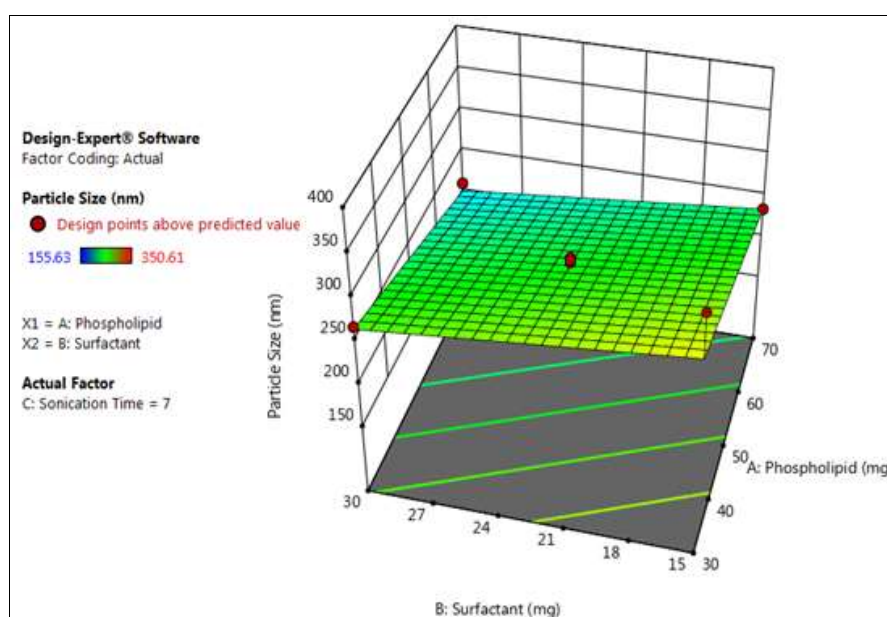
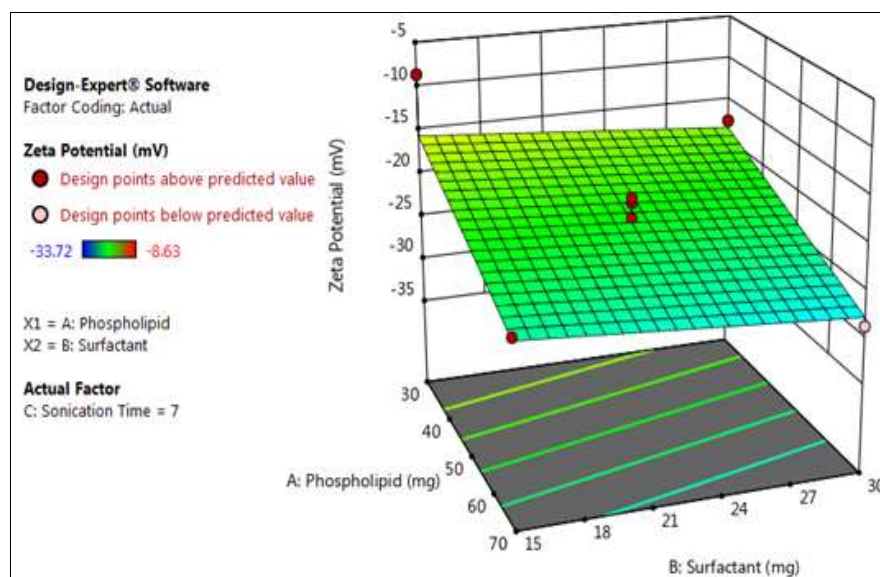
The formulation's initial drug concentration was calculated, and sealed glass ampoules were used to store the medicine. The ampoules were kept at 4 ± 2 °C, 25 ± 2 °C, and 37 ± 2 °C for three months. Samples from each ampoule were tested after 30 days to determine the amount of pharmaceutical leaking. The percent drug loss might be calculated by maintaining the initial drug entrapment at 100% [56].

Results

The results of a 3-factor, 3-level, 12-run BBD generated by Design-Expert software version 11 are displayed. The most optimal concentration of the chosen variables was obtained and formed utilizing the point optimization tool. For each of the 12 formulations, the optimized formulation was assessed for particle size and zeta potential. For repaglinide loaded transferosomes, the responses of the independent variables, particle size and zeta potential, were anticipated. The particle size was determined to be between 155.63 and 350.61 nm. The increase in the number of fatty acid chains in the bilayer structure created by the high phase transition temperature of the phospholipid can be linked to the decrease in particle size at greater concentrations of phospholipids [57]. The model's calculated the F-value of 33.67 implies that it is possibly significant. Only 0.01% of all instances may an F-value this large be caused by noise. When the P-value is less 0.0500, model terms are deemed significant. In this case, key model terms include A, B, and C. If the score is higher than 0.1000, model terms are not significant. If your model contains many extraneous words (apart from those required to maintain hierarchy), model reduction may improve it. The importance of a lack of fit is shown by the F-value of 93.01 for the lack of fit. There is a 0.03% chance that noise contributed to a substantial Lack of Fit F-value. We need the model to fit; significant model fit difficulties are undesirable. Further Zeta Potential for the formulation is found to range from -33.72 to -8.63. In this instance, the model's F-value of 30.63 indicates that it is significant. About 0.01% of all instances may an F-value this large be caused by noise? When the value of the P-value falls beneath 0.0500, model terms are deemed significant. In this case, key model terms include A and C. If the score is higher than 0.1000, the model parameters are not significant. If your model contains many extraneous words (apart from those required to maintain hierarchy), model reduction may improve it. The absence of fit is not significant when compared to the pure error, according to the F-value indicating the lack of fit, which is 1.32. Noise is likely to be the source of a large Lack of Fit F-value in 42.17% of cases. A negligible lack of fit is good because we want the design to fit. A three-dimensional (3D) response surface map was made for the two responses (Y1 and Y2) that shows the linear relationship plots between the actual and predicted values as well as the associated residual plots.

Table 3: Observed responses in Box–Behnken design:

Std	Run	Factor 1 A:Phospholipid mg	Factor 2 B:Surfactant mg	Factor 3 C:Sonication Time min	Response 1 Particle Size nm	Response 2 Zeta Potential mV
10	1	50	30	4	284.52	-11.21
1	2	30	15	7	350.61	-8.63
13	3	50	22.5	7	258.29	-19.52
16	4	50	22.5	7	260.17	-18.94
6	5	70	22.5	4	283.14	-16.34
2	6	70	15	7	234.74	-24.69
3	7	30	30	7	268.54	-17.48
17	8	50	22.5	7	256.89	-21.19
14	9	50	22.5	7	253.71	-25.82
9	10	50	15	4	297.3	-14.72
12	11	50	30	10	172.64	-32.96
7	12	30	22.5	10	195.82	-29.35
4	13	70	30	7	210.03	-28.73
11	14	50	15	10	189.23	-31.6
8	15	70	22.5	10	155.63	-33.72
15	16	50	22.5	7	255.62	-23.26
5	17	30	22.5	4	330.36	-10.2

**Fig 1:** 3D surface graph of Particle Size**Fig 2:** 3D surface graph Zeta Potential

ANOVA for Linear model**Table 4:** Response 1: Particle Size

Source	Sum of Squares	DF	Mean Square	F-value	p-value	
Model	39924.35	3	13308.12	33.67	< 0.0001	significant
A-Phospholipid	8566.75	1	8566.75	21.68	0.0004	
B-Surfactant	2317.10	1	2317.10	5.86	0.0308	
C-Sonication Time	29040.50	1	29040.50	73.48	< 0.0001	
Residual	5137.75	13	395.21			
Lack of Fit	5113.32	9	568.15	93.01	0.0003	significant
Pure Error	24.43	4	6.11			
Cor Total	45062.10	16				

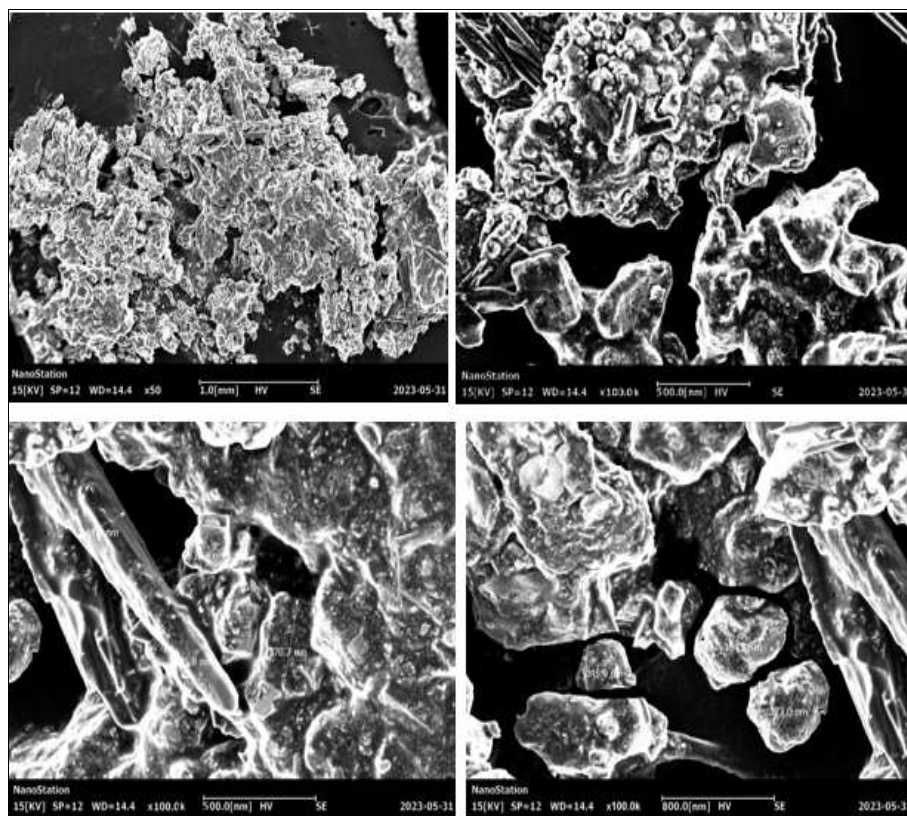
ANOVA for Linear model**Table 5:** Response 2: Zeta Potential

Source	Sum of Squares	DF	Mean Square	F-value	p-value	
Model	899.34	3	299.78	30.63	< 0.0001	significant
A-Phospholipid	178.79	1	178.79	18.27	0.0009	
B-Surfactant	14.42	1	14.42	1.47	0.2464	
C-Sonication Time	706.13	1	706.13	72.16	< 0.0001	
Residual	127.22	13	9.79			
Lack of Fit	95.19	9	10.58	1.32	0.4217	not significant
Pure Error	32.03	4	8.01			
Cor Total	1026.56	16				

Characterization

Morphology: Scanning Electron Microscope (SEM) examination, SEM images of suitable magnifications were

obtained which confirms the shape and size of optimized Repaglinide loaded Transferosomes.

**Fig 3:** SEM Images of F9 transferosomes**Entrapment Efficiency**

The entrapment efficiency is expressed as the proportion of the total amount of drug integrated into the transferosomes to the original drug concentration with the amount of free or

unentrapped amount of drug within the supernatant. It was discovered that the entrapment efficiency of F9 and F7 is higher.

Table 6: % Entrapment Efficiency:

Formulation	% Entrapment Efficiency
F 1	69.28
F 2	70.72
F 3	73.17
F 4	75.68
F 5	68.8
F 6	70.4
F 7	80.58
F 8	71.73
F 9	87.41
F 10	76.26
F 11	78.24
F 12	72.48
F13	74.19
F14	76.32
F15	68.39
F16	71.20
F17	75.25

Particle size, polydispersity index, and zeta potential:

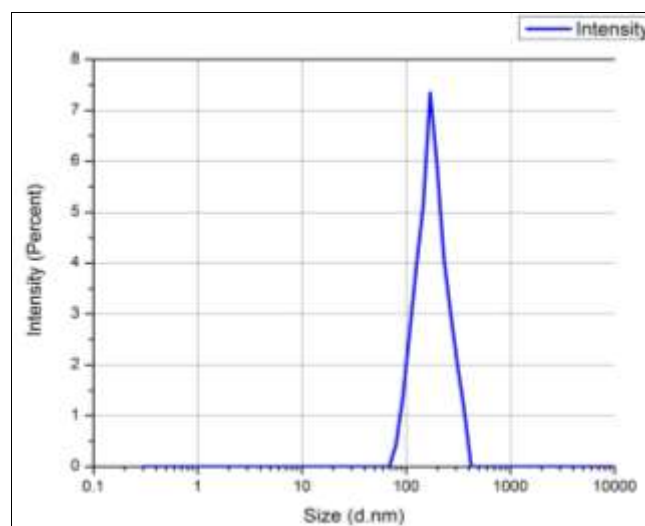
The size of the particles and the zeta potential for multiple transferosome formulations were investigated using the Malvern Zetasizer. Zeta potential is the name for a particle's potential for electricity in a formulation. This parameter

may be used to evaluate the colloidal dispersion's physical stability. In table no. 3.2, the formulations with the highest percentage of entrapment efficacy are listed by zeta potential and particle size.

Table 7: Particle size, polydispersity index, and zeta potential:

Formulation	Particle size (nm)	The Polydispersity index (PDI)	Zeta Potential (mV)
F1	284.52	0.354	-11.21
F2	350.61	0.524	-8.63
F3	258.29	0.763	-19.52
F4	260.17	0.476	-18.94
F5	283.14	0.532	-16.34
F6	234.74	0.617	-24.69
F7	268.54	0.364	-17.48
F8	256.89	0.302	-21.19
F9	253.71	0.456	-25.82
F10	297.3	0.532	-14.72
F11	172.64	0.674	-32.96
F12	195.82	0.325	-29.35
F13	210.03	0.618	-28.73
F14	189.23	0.583	-31.6
F15	155.63	0.421	-33.72
F16	255.62	0.284	-23.26
F17	330.36	0.629	-10.2

Zetasizer Pro (Malvern Instruments GmbH, Herrenberg, Germany) was used to determine the particle size and polydispersity index for the produced repaglinide-loaded transferosomes, and it was discovered that the particle sizes ranged from 155.63 nm to 350.61 nm. Instruments that make use of dynamic light scattering (DLS) can measure the PDI. PDI for the formulation was discovered to range from 0.284 to 0.763. According to international standards organisations (ISOs), monodisperse samples are more likely to have PI values 0.05, whereas samples with a wide size (e.g., polydisperse) distribution of particles are more likely to have values > 0.7 [117]. Therefore, the PDI values we got indicate that the particles are more likely to be monodisperse. Additionally, it was discovered that the formulations F7 and F9 had respective zeta potentials of -29.92 mV and -33.33 mV. The zeta potential value attests to the produced transferosomal suspensions' excellent stability.

**Fig 4:** Graph of particle size of F15

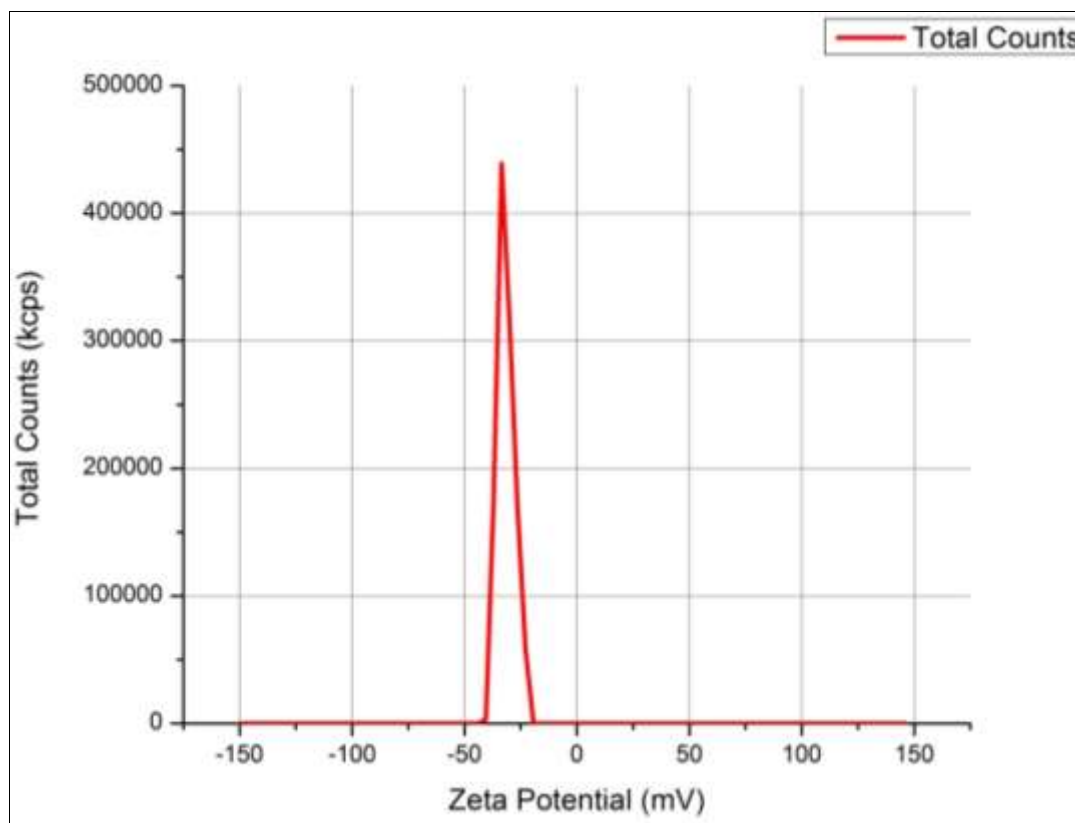


Fig 5: Graph of Zeta Potential of F15

Loading Capacity

Table 8: Loading Capacity:

Formulation	% Loading Capacity:
F 1	40.92
F 2	33.56
F 3	34.32
F 4	35.08
F 5	53.41
F 6	41.31
F 7	44.62
F 8	54.45
F 9	38.43
F 10	55.96
F 11	43.89
F 12	54.71
F13	37.19
F14	42.36
F15	35.65
F16	31.09
F17	48.37

Loading capacity quantifies the amount of drug loaded per unit weight of the nanoparticle and reflects the fraction of the mass of the transfesomes that is attributable to the drug-encapsulated substance. The overall amount of drug entrapped may be estimated by dividing the weight of all the transfesomes by the loading capacity (LC %). It is evident from the preceding table that the formulations F10 and F12, with respective loading capacities of 55.96% and 54.71%, have the maximum loading capacities.

In vitro Drug Release Study

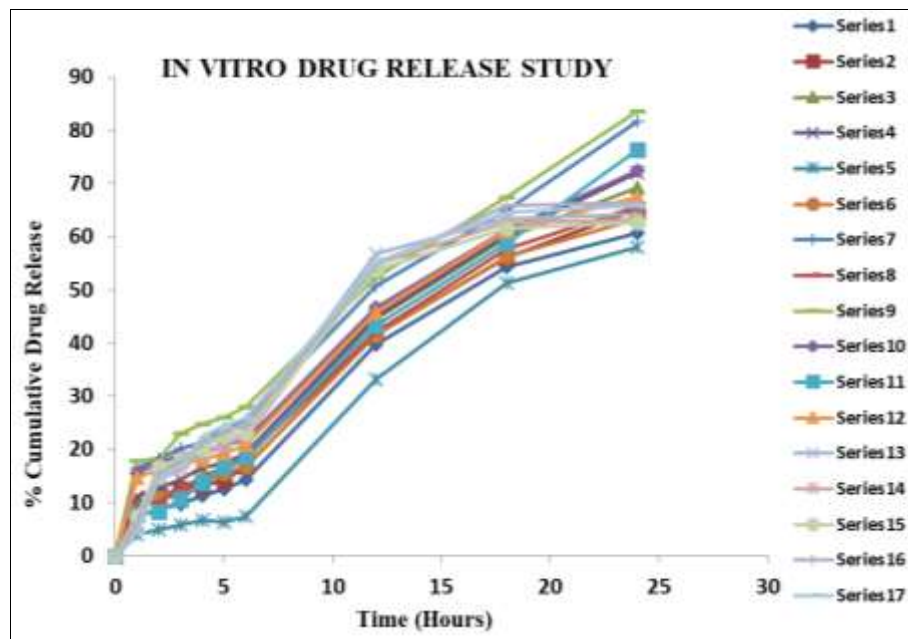
In vitro release studies of Repaglinide loaded Trans ferosomes were performed using egg membrane. The percentage drug release of Repaglinide from Trans ferosomes was studied *in vitro* for about 24 hours. The observation for these studies is reported in the given table.

Table 9: *In vitro* Drug Release Study:

	Formulation	Time (in hours)								
		1	2	3	4	5	6	12	18	24
% Cumulative Drug Release	F1	7.25	8.74	9.78	11.29	12.53	14.36	39.79	54.24	60.67
	F2	9.43	11.41	12.56	13.34	14.12	16.76	41.64	56.14	65.14
	F3	10.24	11.63	12.31	14.98	16.59	18.12	44.47	59.73	69.29
	F4	11.11	12.75	14.24	16.64	17.31	19.31	44.93	60.42	71.98
	F5	3.97	4.84	5.74	6.35	6.67	7.32	33.13	51.37	58.12
	F6	8.64	10.91	11.12	13.58	15.63	16.79	41.48	56.32	63.28
	F7	16.54	18.32	20.16	21.21	23.85	25.45	50.67	64.97	81.72
	F8	9.56	10.02	12.83	14.37	16.19	18.53	42.06	57.65	65.76
	F9	17.84	18.19	22.95	24.76	26.08	27.94	52.34	67.39	83.69
	F10	15.64	17.56	18.99	19.89	20.84	21.74	46.72	61.27	72.44
	F11	7.82	8.32	10.64	13.76	16.72	18.62	43.29	58.76	76.25
	F12	14.69	16.27	17.53	18.11	19.22	20.91	45.76	61.10	67.53
	F13	6.38	15.83	17.92	19.14	20.45	23.53	46.73	58.29	64.24
	F14	5.64	14.37	16.20	18.96	21.42	22.08	44.85	59.63	63.12
	F15	7.32	16.76	18.32	20.20	22.62	23.04	43.84	60.62	62.58
	F16	6.19	15.42	17.76	21.34	23.28	24.54	44.71	61.83	66.36
	F17	4.42	14.62	16.73	22.46	24.52	25.83	45.17	62.56	65.91

The egg membrane was used for the 24-hour *in vitro* drug release test for the transferosomes loaded with repaglinide. For all of the formulations from F1 to F17, cumulative drug

release was determined to be between 53.12% and 83.69% at the 24th hour. The release profiles of both the drugs were shown in Fig.

**Graph 1:** Graph of *in vitro* Drug release profile

Conclusion

The study was conducted to formulate Repaglinide loaded Transferosomes to improve the bioavailability by transdermal route. The Box Behnken design was successfully applied to formulate and optimize the repaglinide loaded transferosomes using “Thin Film Hydration Technique”. The data suggest the significant effect of lipid and Span 80 on entrapment efficiency and drug release. Increase in the lipid content in the transferosomes showed improved entrapment efficiency and improvement in the drug release. From the optimized run of 17, the best formulation is found to be F15 which showed the lowest size of 155.63 nm and highest Zeta Potential of –33.72 mV. Further when checked for entrapment efficiency, F9 showed the highest entrapment efficiency. Also release study follows zero order reaction. The above study confirms

the Repaglinide loaded Transferosomes for their use in diabetes mellitus transdermally and the data obtained may be used further to exploit the dermal route for delivery of the drug. At last, it can be concluded that by using transferosomes as a carrier we can enhance the transdermal delivery of repaglinide and its limitations associated with the conventional dosage form be overcome.

References

- Berná G, Oliveras-López MJ, Jurado-Ruiz E, Tejedo J, Bedoya F, Soria B, *et al.* Nutrigenetics and nutria genomics insights into diabetes etiopathogenesis. *Nutrients*. 2014 Nov 21;6(11):5338-69.
- Silverman BL, Barnes CJ, Campaigne BN, Muchmore DB. Inhaled insulin for controlling blood glucose in

- patients with diabetes. *Vascular Health and Risk Management*. 2007 Dec 1;3(6):947-58.
3. Skovsø S. Modeling type 2 diabetes in rats using high fat diet and streptozotocin. *Journal of diabetes investigation*. 2014 Jul;5(4):349-58.
 4. Rivera-Mancía S, Lozada-García MC, Pedraza-Chaverri J. Experimental evidence for curcumin and its analogs for management of diabetes mellitus and its associated complications. *European Journal of Pharmacology*. 2015 Jun 5;756:30-7.
 5. Hunt KJ, Schuller KL. The increasing prevalence of diabetes in pregnancy. *Obstetrics and gynecology clinics of North America*. 2007 Jun 1;34(2):173-99.
 6. Kanguru L, Bezawada N, Hussein J, Bell J. The burden of diabetes mellitus during pregnancy in low-and middle-income countries: A systematic review. *Global Health Action*. 2014 Dec 1;7(1):23987.
 7. Saedi E, Gheini MR, Faiz F, Arami MA. Diabetes mellitus and cognitive impairments. *World journal of diabetes*. 2016 Sep 9;7(17):412.
 8. Vos T, Flaxman AD, Naghavi M, Lozano R, Michaud C, Ezzati M, *et al*. Years lived with disability (YLDs) for 1160 sequelae of 289 diseases and injuries 1990–2010: a systematic analysis for the Global Burden of Disease Study 2010. *The lancet*. 2012 Dec 15;380(9859):2163-96.
 9. UM OL. Patterns of Management of Diabetic Mellitus and the Outcome in the Enugu State University Teaching Hospital, Enugu, South East Nigeria. 2022;6(1):20-25.
 10. Abdi A, Jalilian M, Sarbarzeh PA, Vlasisavljevic Z. Diabetes and COVID-19: A systematic review on the current evidences. *Diabetes research and clinical practice*. 2020 Aug 1;166:108347.
 11. Tai SY, Lu TH. Why Was COVID-19 Not the First Leading Cause of Death in the United States in 2020? Rethinking the Ranking List. *American journal of public health*. 2021 Dec;111(12):2096-9.
 12. Care D. Economic Costs of Diabetes in the US in 2017. *Diabetes Care*. 2018 May;41:917.
 13. Rekha K, Sinha R. Comparative assessment of meliorative effects of *Syzygium cumuni* and Carica papaya on reproductive physiology of hyperglycemic Mus musculus with respect to male. *Uttar Pradesh journal of zoology*. 2021 Nov 25;42(23):177-85.
 14. Atlas D. International diabetes federation. *IDF Diabetes Atlas, 7th edn*. Brussels, Belgium: International Diabetes Federation; c2015, 33(2).
 15. Ng LC, Gupta M. Transdermal drug delivery systems in diabetes management: A review. *Asian journal of pharmaceutical sciences*. 2020 Jan 1;15(1):13-25.
 16. Falorni A, Minarelli V, Bartoloni E, Alunno A, Gerli R. Diagnosis and classification of autoimmune hypophysitis. *Autoimmunity Reviews*. 2014 Apr 1;13(4-5):412-6.
 17. Culy CR, Jarvis B. Repaglinide: A review of its therapeutic use in type 2 diabetes mellitus. *Drugs*. 2001 Sep;61(11):1625-60.
 18. Marbury T, Huang WC, Strange P, Lebovitz H. Repaglinide versus glyburide: A one-year comparison trial. *Diabetes research and clinical practice*. 1999 Mar 1;43(3):155-66.
 19. Mandić Z, Gabelica V. Ionization, lipophilicity and solubility properties of repaglinide. *Journal of pharmaceutical and biomedical analysis*. 2006 Jun 7;41(3):866-71.
 20. Gertz M, Harrison A, Houston JB, Galetin A. Prediction of human intestinal first-pass metabolism of 25 CYP3A substrates from *in vitro* clearance and permeability data. *Drug Metabolism and Disposition*. 2010 Jul 1;38(7):1147-58.
 21. Pakkiri Maideen NM, Manavalan G, Balasubramanian K. Drug interactions of meglitinides antidiabetic involving CYP enzymes and OATP1B1 transporter. *Therapeutic advances in endocrinology and metabolism*. 2018 Aug;9(8):259-68.
 22. Sachan R, Bajpai M. Transdermal drug delivery system: A review.
 23. Rizwan M, Aqil M, Talegaonkar S, Azeem A, Sultana Y, Ali A, *et al*. Enhanced transdermal drug delivery techniques: An extensive review of patents. *Recent patents on drug delivery & formulation*. 2009 Jun 1;3(2):105-24.
 24. Lu K, Xie S, Han S, Zhang J, Chang X, Chao J, *et al*. Preparation of a nano emodin transfersome and study on its anti-obesity mechanism in adipose tissue of diet-induced obese rats. *Journal of translational medicine*. 2014 Dec;12(1):1-4.
 25. Loo CH, Basri M, Ismail R, Lau HL, Tejo BA, Kanthimathi MS, *et al*. Effect of compositions in nanostructured lipid carriers (NLC) on skin hydration and occlusion. *International journal of nanomedicine*. 2012 Dec 27:13-22.
 26. Song SH, Lee KM, Kang JB, Lee SG, Kang MJ, Choi YW. Improved skin delivery of voriconazole with a nanostructured lipid carrier-based hydrogel formulation. *Chemical and Pharmaceutical Bulletin*. 2014 Aug 1;62(8):793-8.
 27. Chen-yu G, Chun-fen Y, Qi-lu L, Qi T, Yan-wei X, Wei-na L, *et al*. Development of a quercetin-loaded nanostructured lipid carrier formulation for topical delivery. *International journal of pharmaceutics*. 2012 Jul 1;430(1-2):292-8.
 28. Walve JR, Bakliwal SR, Rane BR, Pawar SP. Transfersomes: A surrogated carrier for transdermal drug delivery system; c2011.
 29. Sivannarayana P, Rani AP, Saikishore V, Venu Babu C, Sri Rekha V. Transfersomes: Ultra deformable vesicular carrier systems in transdermal drug delivery system. *Research Journal of Pharmaceutical Dosage Forms and Technology*. 2012;4(5):243-55.
 30. Sachan R, Parashar T, Soniya SV, Singh G, Tyagi S, Patel C, *et al*. Drug carrier transfersomes: A novel tool for transdermal drug delivery system. *International Journal of Research and Development in Pharmacy and Life Sciences*. 2013 Feb;2(2):309-16.
 31. Li J, Wang X, Zhang T, Wang C, Huang Z, Luo X, *et al*. A review on phospholipids and their main applications in drug delivery systems. *Asian journal of pharmaceutical sciences*. 2015 Apr 1;10(2):81-98.
 32. Bhasin B, Londhe VY. An overview of transfersomal drug delivery. *Int. J Pharm. Sci. Res*. 2018 Jun 1;9(6):2175-84.
 33. Lei W, Yu C, Lin H, Zhou X. Development of tacrolimus-loaded transfersomes for deeper skin penetration enhancement and therapeutic effect improvement *in vivo*. *Asian journal of pharmaceutical sciences*. 2013 Dec 1;8(6):336-45.

34. Pandey A, Mittal A, Chauhan N, Alam S. Role of surfactants as penetration enhancer in transdermal drug delivery system. *J Mol Pharm Org Process Res.* 2014;2(113):2-7.
35. Som I, Bhatia K, Yasir M. Status of surfactants as penetration enhancers in transdermal drug delivery. *Journal of pharmacy & bioallied sciences.* 2012 Jan;4(1):2.
36. Aggarwal N, Goindi S. Preparation and evaluation of antifungal efficacy of griseofulvin loaded deformable membrane vesicles in optimized guinea pig model of *Microsporum canis*-Dermatophytosis. *International journal of pharmaceutics.* 2012 Nov 1;437(1-2):277-87.
37. Chen J, Lu WL, Gu W, Lu SS, Chen ZP, Cai BC. Skin permeation behavior of elastic liposomes: role of formulation ingredients. *Expert opinion on drug delivery.* 2013 Jun 1;10(6):845-56.
38. Duangjit S, Opanasopit P, Rojanarata T, Ngawhirunpat T. Effect of edge activator on characteristic and *in vitro* skin permeation of meloxicam loaded in elastic liposomes. *Advanced Materials Research.* 2011 Apr 20;194:537-40.
39. Jacob L, Anoop KR. A review on surfactants as edge activators in ultradeformable vesicles for enhanced skin delivery. *Int J Pharm Bio Sci.* 2013;4(3):337-44.
40. Kim B, Cho HE, Moon SH, Ahn HJ, Bae S, Cho HD, *et al.* Transdermal delivery systems in cosmetics. *Biomedical Dermatology.* 2020 Dec;4:1-2.
41. Kumar GP, Rajeshwarrao P. Nonionic surfactant vesicular systems for effective drug delivery—an overview. *Acta pharmaceutical Sinica B.* 2011 Dec 1;1(4):208-219.
42. Mathur M, Sundaramoorthy S. Anticancer herbal drugs and their improvement through novel drug delivery approaches. *Applied Biological Research.* 2013;15(1):1-20.
43. Pawar AY. Transfersome: A novel technique which improves transdermal permeability. *Asian Journal of Pharmaceutics (AJP).* 2016 Dec 21;10(04).
44. Ghai I, Chaudhary H, Ghai S, Kohli K, Kr V. A review of transdermal drug delivery using nano-vesicular carriers: Transfersomes. *Recent Patents on Nanomedicine.* 2012 Oct 1;2(2):164-71.
45. Vinod KR, Kumar MS, Anbazhagan S, Sandhya S, Saikumar P, Rohit RT, *et al.* Critical issues related to transfersomes-novel vesicular system. *Acta Scientiarum Polonorum Technologia Alimentaria.* 2012 Mar 30;11(1):67-82.
46. Gupta V, Trivedi P. Enhancement of storage stability of cisplatin-loaded protransfersome topical drug delivery system by surface modification with block copolymer and gelling agent. *Journal of drug delivery science and technology.* 2012 Jan 1;22(4):361-6.
47. Jiang T, Wang T, Li T, Ma Y, Shen S, He B, *et al.* Enhanced transdermal drug delivery by transfersome-embedded oligopeptide hydrogel for topical chemotherapy of melanoma. *ACS nano.* 2018 Sep 5;12(10):9693-701.
48. Chauhan P, Tyagi BK. Herbal novel drug delivery systems and transfersomes. *Journal of Drug Delivery and Therapeutics.* 2018 May 14;8(3):162-8.
49. Garg V, Singh H, Bimbrawh S, Kumar Singh S, Gulati M, Vaidya Y, *et al.* Ethosomes and transfersomes: Principles, perspectives and practices. *Current drug delivery.* 2017 Aug 1;14(5):613-33.
50. Moawad FA, Ali AA, Salem HF. Nanotransfersomes-loaded thermosensitive in situ gel as a rectal delivery system of tizanidine HCl: preparation, *in vitro* and *in vivo* performance. *Drug delivery.* 2017 Jan 1;24(1):252-60.
51. Ramkanth S, Anitha P, Gayathri R, Mohan S, Babu D. Formulation and design optimization of nanotransfersomes using pioglitazone and eprosartan mesylate for concomitant therapy against diabetes and hypertension. *European Journal of Pharmaceutical Sciences.* 2021 Jul 1;162:105811.
52. Almeahady AM, Elsis AM. Development, optimization, and evaluation of tamsulosin nanotransfersomes to enhance its permeation and bioavailability. *Journal of Drug Delivery Science and Technology.* 2020 Jun 1;57:101667.
53. Gupta A, Aggarwal G, Singla S, Arora R. Transfersomes: a novel vesicular carrier for enhanced transdermal delivery of sertraline: development, characterization, and performance evaluation. *Scientia pharmaceutica.* 2012 Dec;80(4):1061-80.
54. Xu L, Pan J, Chen Q, Yu Q, Chen H, Xu H, *et al.*, *In vivo* evaluation of the safety of triptolide-loaded hydrogel-thickened microemulsion. *Food and chemical toxicology.* 2008;46(12):3792-3799.
55. Opatha SA, Titapiwatanakun V, Chutoprapat R. Transfersomes: A promising nanoencapsulation technique for transdermal drug delivery. *Pharmaceutics.* 2020 Sep;12(9):855.
56. Khan I, Needham R, Yousaf S, Houacine C, Islam Y, Bnyan R, *et al.* Impact of phospholipids, surfactants and cholesterol selection on the performance of transfersomes vesicles using medical nebulizers for pulmonary drug delivery. *Journal of Drug Delivery Science and Technology.* 2021 Dec 1;66:102822.
57. El Zaafarany GM, Awad GA, Holayel SM, Mortada ND. Role of edge activators and surface charge in developing ultra-deformable vesicles with enhanced skin delivery. *International journal of pharmaceutics.* 2010 Sep 15;397(1-2):164-72.